S1 Comparison between PTR-TOF-MS and GC-MS measurements of isoprene and the sum of the monoterpenes

A comparison between the GC-MS and PTR-TOF-MS results for isoprene and the sum of the monoterpenes can be found in the Figures S1 and S2. PTR-TOF-MS data with a 1 min time resolution were merged onto the 20 min sampling time of the GC-MS. The dashed lines in these figures refer to a time period where a contamination in the PTR-TOF-MS is assumed. This period was excluded from the comparison. During the day the isoprene data measured by the PTR-TOF-MS were ca. 1.4 times higher than the GC-MS data (Figure S1), while at the low level nighttime values the PTR-TOF-MS system measured ca. 7.5 times more isoprene than the GC-MS (determined from diel median values over the whole campaign). An insufficient determination of the humidity dependency of the PTR-TOF-MS for isoprene can be ruled out as a possible explanation, because isoprene measurements are not dependent on humidity (see section 2.2.1). A possible reason for the discrepancy could be a minor interference between 2-methyl-3-buten-2-ol (MBO) which is emitted by vegetation (Kesselmeier and Staudt, 1999) and isoprene within the PTR-TOF-MS. A fragment of MBO is measured on the same mass as isoprene (e.g. Park et al., 2013). Although significant MBO emissions have been detected only in North America (e.g. Harley et al., 1998; Goldan et al., 1993), a contribution from Mediterranean vegetation cannot be excluded. A correlation of the two data sets (PTR vs. GC data) using a bivariate fit algorithm resulted in a slope of 1.2, an intercept of 10.9 pptv and a r^2 value of 0.89 (see Fig. S3). The data were color coded by the date and time of the recording. It becomes clear that the agreement between the two data sets varied slightly with time. Thus, an instrumental issue during a specific period cannot be ruled out. The lower part of Figure S2 shows the data of α-pinene, the sum of β-pinene and Δ3-carene as well as limonene measured by the GC-MS system. The sum of the monoterpenes measured by GC-MS are compared to the total monoterpene signal measured by PTR-TOF-MS at 137.13 amu in the upper part. The PTR-TOF-MS data are up to 2.4 times higher than the GC data (determined from diel median values over the whole campaign). This can partly be explained by the fact that the sum on mass 137 amu can also contain monoterpenes other than those quantified by the GC-MS. The correlation between the two signals (bivariate fit algorithm, PTR vs. GC) leads to a slope of 1.6, an intercept of 0.99 pptv and a correlation coefficient $r^2 = 0.82$ (see Fig. S4). This is reasonable given unmeasured monoterpenes by GC-MS. Furthermore, the total monoterpene signal of the PTR-TOF-MS system was calibrated with α-pinene. Thus, slight differences in sensitivity, which occur as soon as α-pinene is not the dominant species, can play a role.

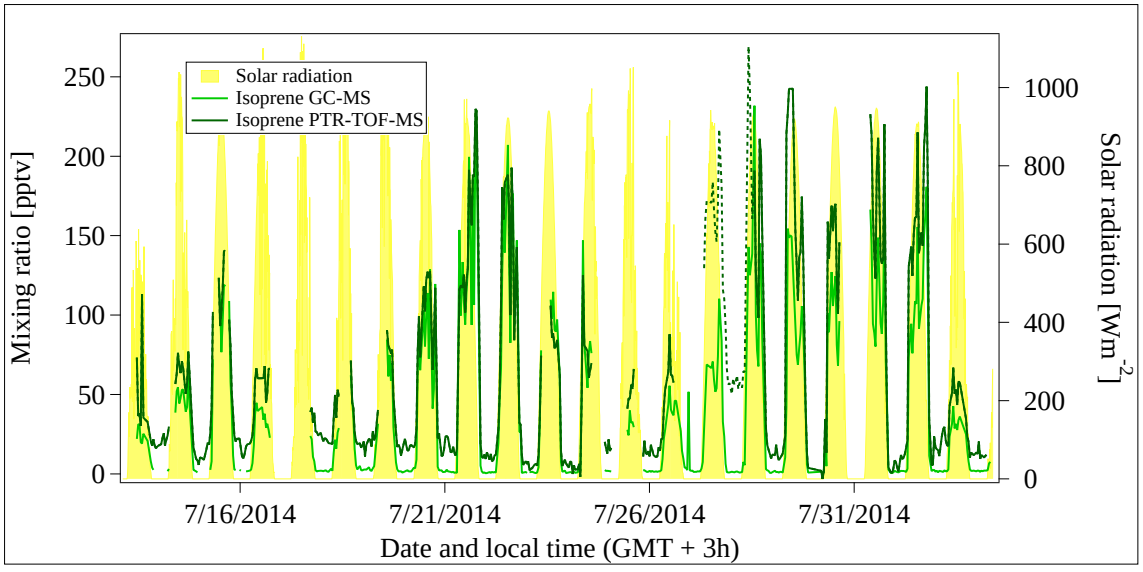

Figure S1. Time traces of isoprene in pptv measured by GC-MS and PTR-TOF-MS as well as solar radiation in Wm^{-2}. The PTR-TOF-MS data with a time resolution of 1 min were merged on the 20 minute sampling time of the GC-MS. Solar radiation is shown in a 10 min time resolution. The dashed line marks a possible contamination in the PTR-TOF-MS data.

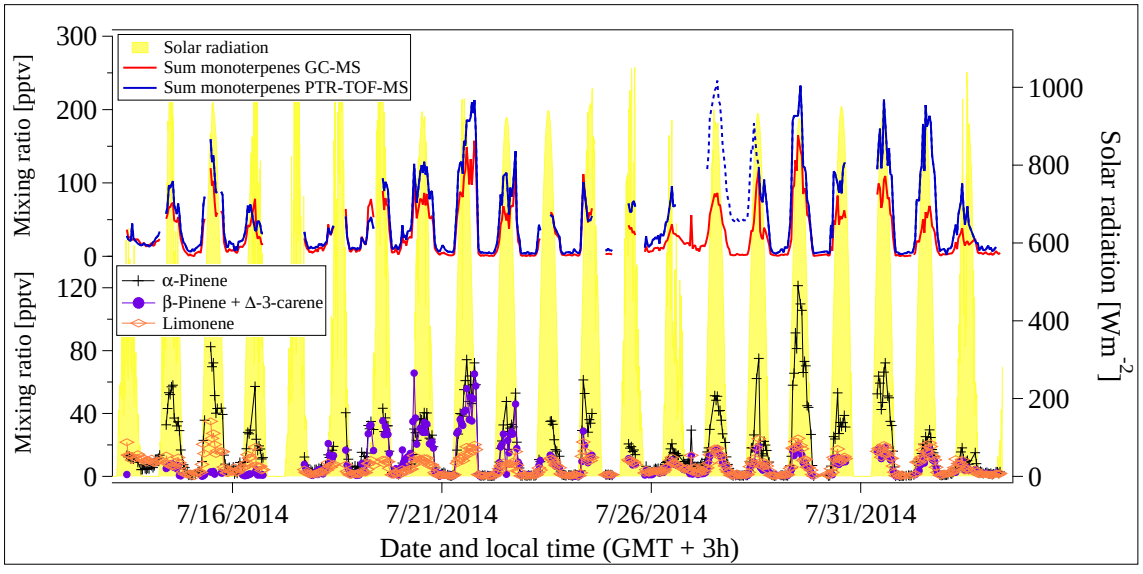

Figure S2. Time traces of different monoterpenes in pptv as well as solar radiation in Wm^{-2}. The PTR-TOF-MS data with a time resolution of 1 min were merged on the 20 minute sampling time of the GC-MS. Solar radiation is shown in a 10 min time resolution. The upper part shows the sum of the monoterpenes measured by GC-MS and PTR-TOF-MS, the lower part displays individual monoterpenes measured by GC-MS, only. The dashed line marks a possible contamination in the PTR-TOF-MS data.

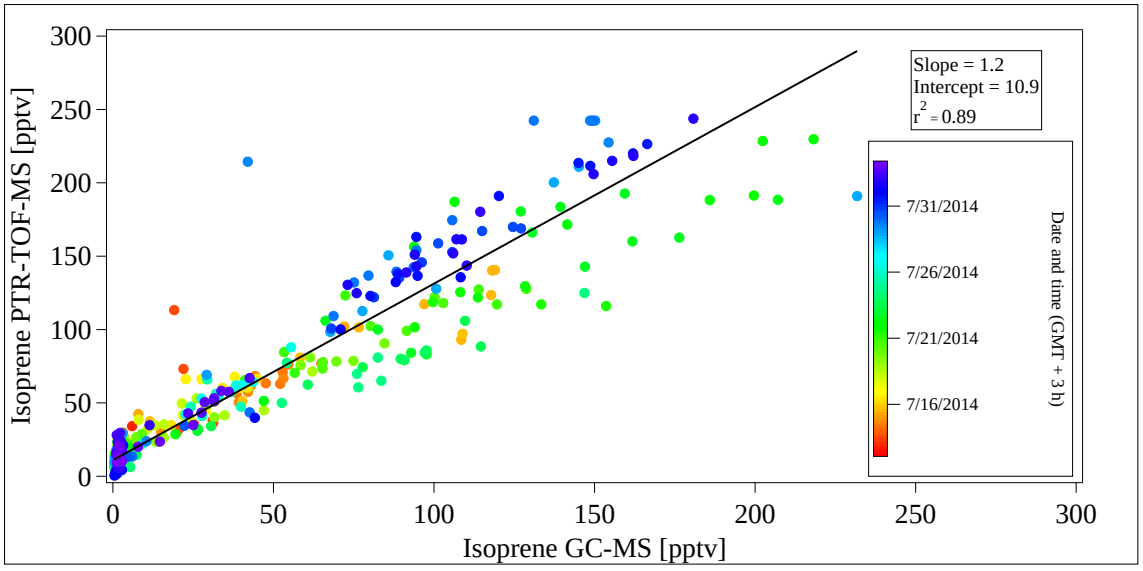

Figure S3. Isoprene data measured by PTR-TOF-MS plotted against isoprene values measured by GC-MS. A bivariate fitting algorithm was applied. The data were color coded by the date and time of recording.

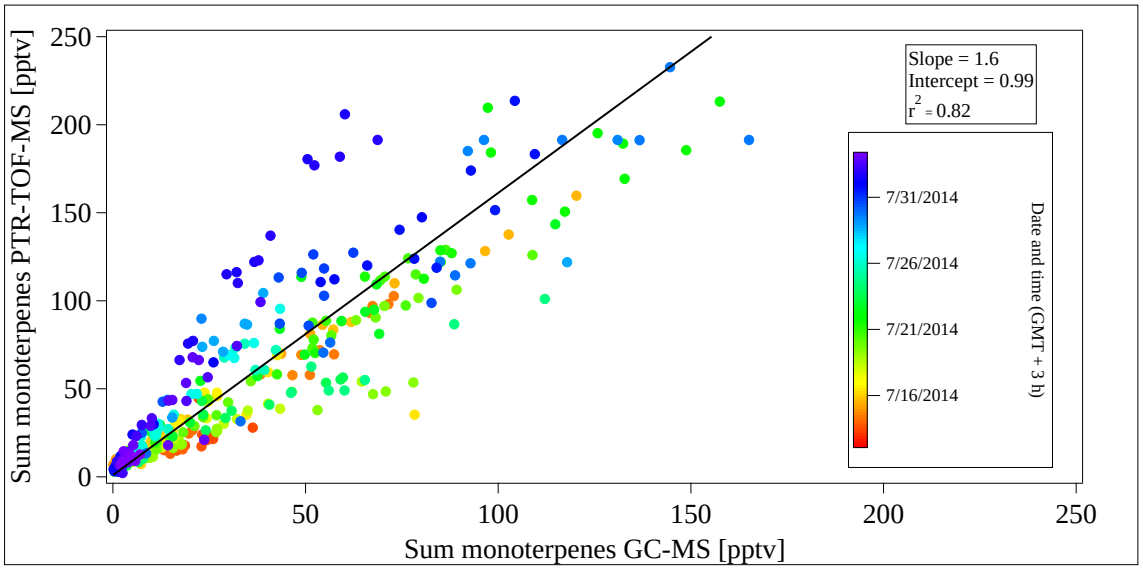

Figure S4. The sum of the monoterpenes measured by PTR-TOF-MS plotted against the sum of α-pinene, β-pinene, Δ-carene and limonene measured by GC-MS. A bivariate fitting algorithm was applied. The data were color coded by the date and time of recording.

S2 Onset of the sea breeze

To exemplify the onset of the sea breeze, isoprene from 22 July has been plotted at 1 minute time resolution in Figure S5. On that day at around 9:30 am local time the wind changed from N-NE to W-SW direction which was accompanied by a sharp increase in relative humidity and in atmospheric dimethyl sulfide (DMS), a species primarily emitted from marine sources (Cline and Bates, 1983; Mesarchaki et al., 2014). Prior to the change in wind direction, the isoprene mixing ratio began increasing with temperature as expected. However, as soon as the local sea breeze set-in and the wind direction changed abruptly to the west, the isoprene levels decreased leaving an early morning spike. The apparent peak in isoprene at ca. 10:00 am is therefore generated by the wind change combined with the shorter section of isoprene emitting vegetated land between the site and the coast when the wind is from the west. This behavior is consistent with the current understanding that the sea is only a weak source of isoprene and the main source is the local terrestrial vegetation (Bonsang et al., 1992; Broadgate et al., 1997; Palmer and Shaw, 2005; Arnold et al., 2009).
In this study DMS was only used qualitatively, because a comparison between the DMS measurements of the PTR-TOF-MS and the GC-MS instrument revealed a large discrepancy. One possible reason was that the catalytic converter of the PTR-TOF-MS used for background measurements emitted small quantities of DMS, so that the DMS background could not be determined accurately. Therefore the baseline next to the peak was applied as background signal.

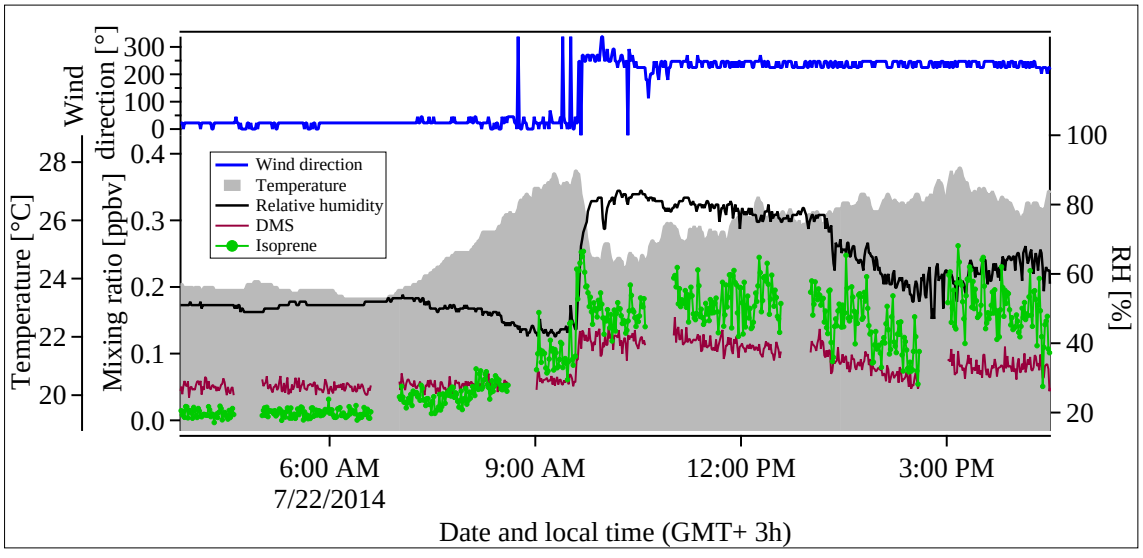

Figure S5. Mixing ratios of isoprene and DMS in ppbv as well as wind direction in °, temperature in °C and relative humidity in % as a function of time with a 1 minute time resolution.

S3 Initial values in the CAABA/MECCA box model

Compound	Initial value in ppbv
nC_4H_{10}	0.2
NH_3	8
C_2H_6	0.9
C_3H_8	0.5
iC_4H_{10}	0.09
C_2H_2	0.3
Toluene	0.1
CH_3CO_3H	0.04
Benzene	0.05
CH_4	1800
Xylenes	0.09
Ethylbenzene	0.01
Trimethylbenzenes	0.009
$C_{11}H_{14}$ (LHAROM)	0.008
CH_3CO_2H	0.3
CH_3CN	0.01
PAN	0.2
CH_3OOH	0.25
HCN	0.07
MBO	0.002
Methylpropene	0.006
β-Pinene	0.03
Sabinene	0.006
Camphene	0.005

Compound	Initial value in ppbv
α-Pinene	0.025
Carene	0.004
HONO	0.009
cBut-2-ene	0.004
tBut-2-ene	0.003
CH_3OH	3
Styrene	0.003
H_2O_2	1.8
CH_3COCH_3	1
C_5H_8	0.5
HNO_3	0.8
Hydroxyacetone (Acetol)	0.35
Glyoxal	0.06
Methylglyoxal	0.1
CH_3CHO	0.4
$HOCH_2CHO$	0.25
HCOOH	0.25
CO	100
O_3	50
NO_2	2
NO	0.4
HCHO	2
O_2	2.1×10^8
N_2	7.8×10^8
CO_2	4×10^5

S4 Figures showing the rates of important reactions with a production or loss rate $\geq 10^{-16}$ mol mol^{-1} s^{-1} (0.36 pptv/h) for methanol and acetone

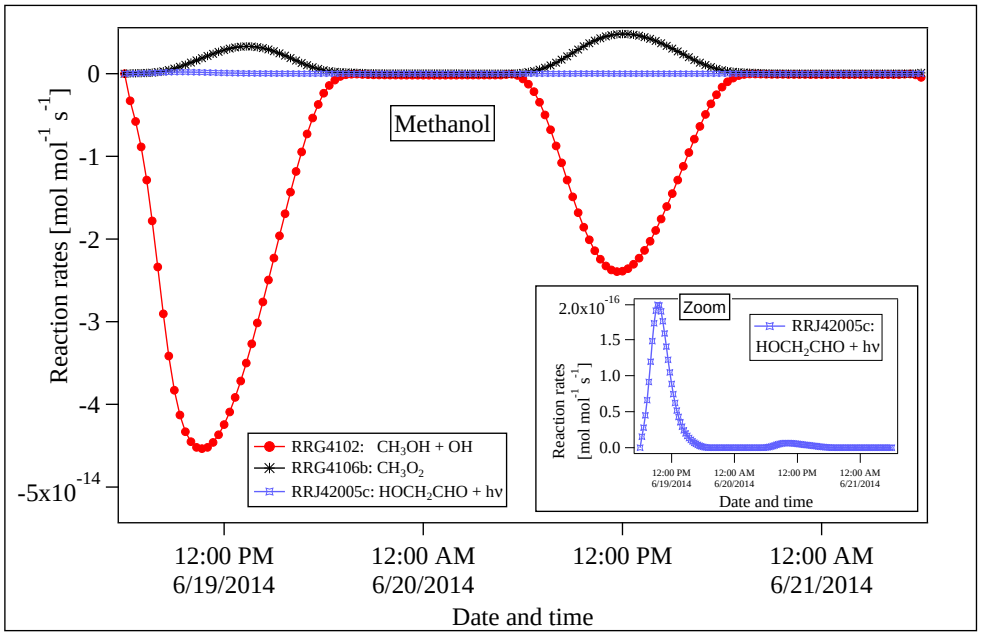

Figure S6. Rates for reactions influencing the mixing ratio of methanol. Further explanation of the reactions can be found in S4.

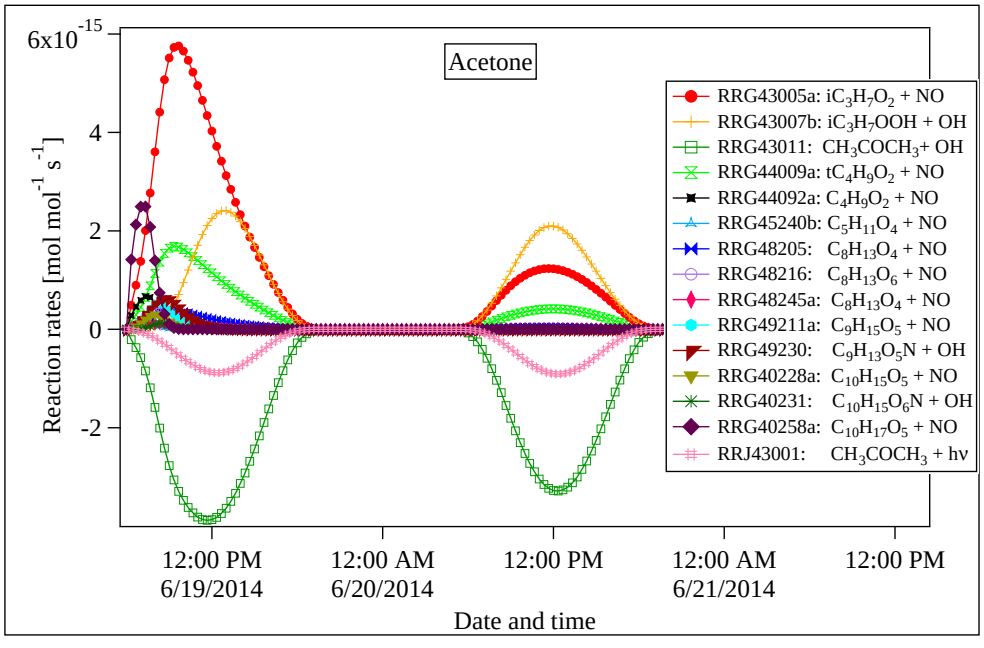

Figure S7. Rates for reactions influencing the mixing ratio of acetone. Further explanation of the reactions can be found in S4.

References

Arnold, S. R., Spracklen, D. V., Williams, J., Yassaa, N., Sciare, J., Bonsang, B., Gros, V., Peeken, I., Lewis, A. C., Alvain, S., and Moulin, C.: Evaluation of the global oceanic isoprene source and its impacts on marine organic carbon aerosol, Atmos. Chem. Phys., 9, 1253–1262, doi:10.5194/acp-9-1253-2009, http://www.atmos-chem-phys.net/9/1253/2009/, 2009.

Bonsang, B., Polle, C., and Lambert, G.: Evidence for marine production of isoprene, Geophys. Res. Lett., 19, 1129–1132, doi:10.1029/92GL00083, http://dx.doi.org/10.1029/92GL00083, 1992.

Broadgate, W. J., Liss, P. S., and Penkett, S. A.: Seasonal emissions of isoprene and other reactive hydrocarbon gases from the ocean, Geophys. Res. Lett., 24, 2675–2678, doi:10.1029/97GL02736, http://dx.doi.org/10.1029/97GL02736, 1997.

Cline, J. D. and Bates, T. S.: Dimethyl sulfide in the Equatorial Pacific Ocean: A natural source of sulfur to the atmosphere, Geophys. Res. Lett., 10, 949–952, doi:10.1029/GL010i010p00949, http://dx.doi.org/10.1029/GL010i010p00949, 1983.

Goldan, P. D., Kuster, W. C., Fehsenfeld, F. C., and Montzka, S. A.: The observation of a C5 alcohol emission in a North American pine forest, Geophys. Res. Lett., 20, 1039–1042, doi:10.1029/93GL00247, http://dx.doi.org/10.1029/93GL00247, 1993.

Harley, P., Fridd-Stroud, V., Greenberg, J., Guenther, A., and Vasconcellos, P.: Emission of 2-methyl-3-buten-2-ol by pines: A potentially large natural source of reactive carbon to the atmosphere, J. Geophys. Res. - Atmos., 103, 25 479–25 486, doi:10.1029/98JD00820, http://dx.doi.org/10.1029/98JD00820, 1998.

Kesselmeier, J. and Staudt, M.: Biogenic Volatile Organic Compounds (VOC): An Overview on Emission, Physiology and Ecology, J. Atmos. Chem., 33, 23–88, doi:10.1023/A:1006127516791, http://dx.doi.org/10.1023/A%3A1006127516791, 1999.

Mesarchaki, E., Yassaa, N., D., H., Lutterbeck, H. E., Zindler, C., and Williams, J.: A novel method for the measurement of VOCs in seawater using needle trap devices and GC–MS, Mar. Chem., 149, 1–8, doi:10.1016/j.marchem.2013.12.001, http://www.sciencedirect.com/science/article/pii/S0304420313002077, 2014.

Palmer, P. I. and Shaw, S. L.: Quantifying global marine isoprene fluxes using MODIS chlorophyll observations, Geophys. Res. Lett., 32, doi:10.1029/2005GL022592, http://dx.doi.org/10.1029/2005GL022592, 2005.

Park, J.-H., Goldstein, A. H., Timkovsky, J., Fares, S., Weber, R., Karlik, J., and Holzinger, R.: Eddy covariance emission and deposition flux measurements using proton transfer reaction–time of flight–mass spectrometry (PTR-TOF-MS): comparison with PTR-MS measured vertical gradients and fluxes, Atmos. Chem. Phys., 13, 1439–1456, doi:10.5194/acp-13-1439-2013, http://www.atmos-chem-phys.net/13/1439/2013/, 2013.